Heliyon 10 (2024) e32042

Contents lists available at ScienceDirect

Heliyon

journal homepage: www.cell.com/heliyon

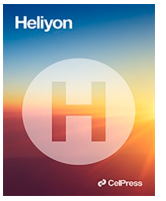

Research article

Kinematic synergies show good consistency when extracted with a low-cost markerless device and a marker-based motion tracking system

Cristina Brambilla *, Alessandro Scano

Institute of Intelligent Industrial Systems and Technologies for Advanced Manufacturing (STIIMA), Italian Council of National Research (CNR), Milano, Italy

ARTICLE INFO

Keywords:
Motor control
Kinematic synergies
Kinect
Vicon
Mixed matrix factorization

ABSTRACT

Recently, markerless tracking systems, such as RGB-Depth cameras, have spread to overcome some of the limitations of the gold standard marker-based tracking systems. Although these systems are valuable substitutes for human motion analysis, as they guarantee higher flexibility, faster setup time and lower costs, their tracking accuracy is lower with respect to marker-based systems. Many studies quantified the error made by markerless systems in terms of body segment length estimation, articular angles, and biomechanics, concluding that they are appropriate for many clinical applications related to motion analysis. We propose an innovative approach to compare a markerless tracking system (Kinect V2) with a gold standard marker-based system (Vicon), based on motor control assessment. We quantified kinematic synergies from the tracking data of fifteen participants performing multi-directional upper limb movements. Kinematic synergy analysis decomposes the kinematic data into a reduced set of motor primitives that describe how the central nervous system coordinates motion at spatial and temporal level. Synergies were extracted with the recently released mixed-matrix factorization algorithm. Four synergies were extracted from both marker-based and markerless datasets and synergies were grouped in 6 clusters for each dataset. Cosine similarity in each cluster was $\geqslant$0.60 in both systems, showing good consistency of synergies. Good matching was found between synergies extracted from markerless and from marker-based data, with a cosine similarity between matched synergies $\geqslant$0.60 in 5 out 6 synergies. These results showed that the markerless sensor can be feasible for kinematic synergy analysis for gross movements, as it correctly estimates the number of synergies and in most cases also their spatial and temporal organization.

1. Introduction

Human motion tracking is a fundamental assessment for analyzing movement kinematics in various scenarios, such as investigating pathological conditions in clinics. Markerless tracking systems, including RGB-Depth cameras and inertial measurements systems (IMUs), are recently-developed technologies that are used for human motion tracking. In the last decade, these technologies have spread to overcome some of the limitations of the gold standard marker-based tracking systems. Indeed, marker-based systems consist

* Corresponding author. Institute of Intelligent Industrial Systems and Technologies for Advanced Manufacturing (STIIMA), Italian Council of National Research (CNR), Via A. Corti 12, 20133, Milan, Italy.
E-mail addresses: cristina.brambilla@stiima.cnr.it (C. Brambilla), alessandro.scano@stiima.cnr.it (A. Scano).

https://doi.org/10.1016/j.heliyon.2024.e32042
Received 12 March 2024; Received in revised form 23 May 2024; Accepted 27 May 2024
Available online 28 May 2024

in a set of infrared cameras that register the 3D position of markers that are attached to anatomical landmarks of the human body. They are characterized by a very high tracking accuracy (error in 3D positioning <1 mm). However, these systems are expensive, require large setups in laboratories and long preparation times. Therefore, markerless systems became a valuable alternative for human motion analysis in many applications as they provide higher flexibility, faster setups and lower costs [1]. However, markerless systems such as Kinect cameras that are based on a combination of RGB and depth sensors, were originally conceived for entertainment purposes and, therefore, they are less accurate than the marker-based systems. Despite this limitation, Kinect cameras have been employed for a wide variety of applications, such as human action recognition [2] and human 3D reconstruction [3], and they became very popular in the rehabilitation and clinical scenarios since they have much lower costs and are easily useable. Indeed, the increasing need of clinical assistance and rehabilitation have stressed the lack of staffs and structures and the high costs related to rehabilitation, especially in clinical environment [4]. At the same time, the growing sanitary costs and events such as the COVID 19 pandemic crisis led to the necessity of telerehabilitation and home monitoring. In this scenario, markerless systems represent a cost-effective and portable solution that guarantees patient monitoring and evaluation at home [5–7], leading to many Kinect-based setups. In this way, delivering therapies at home reduces the costs and improve the accessibility and efficiency of the rehabilitation and to guarantee the continuity of care. Indeed, Kinect cameras have been used in clinical practice for evaluating movement performance in post-stroke patients in upper limb [8]. The Kinect sensors demonstrated to be feasible in many clinical or medical care scenarios including lower limb for evaluating stroke patients [9], patients with multiple sclerosis [10] and in complex clinical applications, like measuring clinically relevant movements in patients with Parkinson's disease [11].

An extensive use of markerless system requires the understanding of their tracking capabilities and limitations. In literature, many studies investigated the reliability of the Kinect cameras with respect to gold standard systems. Clark et al. studied postural control and balance, finding excellent results with both Kinect V1 [12] and V2 [13]. Many studies analyzed the Kinect accuracy when computing spatiotemporal gait parameters, showing good agreement with the marker-based systems with all the generations of Kinect cameras [14–16]. However, in few other studies, the accuracy of joint kinematics was put into discussion [17] and upper limbs [18] was poor, especially for distal joints, such as wrist or ankle, and for tracking fine movements [11,19]. Moreover, the accuracy of Kinect cameras decreases when some parts of the body are hidden [20,21]. Although the studies available are in most cases very comprehensive, they mostly investigated "standard" kinematic parameters, such as 3D joint positions, segment lengths, or articular kinematics. Only in few studies, the analysis was extended to biomechanics with joint torques [22] and normalized jerk [23], finding that Kinect cameras are in general suitable for assessing biomechanics. To the best of our knowledge, very few studies [24,25] have analyzed the capability of Kinect cameras when considering the control of motor coordination of multiple degrees of freedom that can be assessed with a multi-joint synergistic approach i.e., kinematic synergies. Kinematic synergies are the kinematic dual of muscle synergies, a quantitative framework for motor control based on the hypothesis that the central nervous system (CNS) controls multiple degrees of freedom (DoF) through a combination of motor primitives, called synergies, rather than with separate commands. So far coupled only with marker-based tracking systems, kinematic synergy analysis has been already used for the motor control of hand posture and grasps [26–28], human locomotion [29], and upper limb movements [30]. The most diffused synergy model (spatial synergy model) decomposes the kinematic signal in spatial time-invariant synergies and in corresponding temporal activations that activate each synergy differently for every motor task. The factorization algorithms that are usually employed are the non-negative matrix factorization (NMF) algorithm [31] for muscle synergies and the principal component analysis (PCA) for kinematic synergies. PCA allows to decompose signals with positive and negative components; however, with respect to NMF, PCA adds the constraint of orthogonality between synergies, which does not reflect any physiologically relevant constrain. Recently, the new mixed-matrix factorization (MMF) algorithm [32] was released for decomposing muscle and kinematic signals together, allowing to factorize positive and negative signals without the constraint of orthogonality. The MMF algorithm decomposes the input signal into synergies with positive and negative components and corresponding non-negative temporal coefficients. It has been employed for the extraction of kinematic-muscle synergies for the upper limb [32] and for hand grasps [33], and it can be applied to any unconstrained signal. Therefore, it can be used for the extraction of kinematic synergies. The synergistic control aims at understanding how the degrees of freedom are coordinated to achieve purposeful movement. There is plenty of literature regarding muscle and/or kinematic synergies that suggests that assessing synergies is a method to quantify motor control and coordination. The changes in the modular organization of the neuro-motor system, expressed in terms of number, structure and recruitment of synergies, is a long-established concept in rehabilitation, allowing to discriminate a variety of pathological changes in the nervous system [34]. Synergies describe the underlying modular organization of the motor control that in neurological patients. Restoring synergistic control should be the main focus of rehabilitation [35] as motor modules are at the basis of motor control [36] and cannot be assessed by using standard kinematic measures, such as range of motion (ROM) and smoothness metrics. The recovery of physiological motor modules provides evidence of motor recovery and, therefore, kinematic synergy analysis adds a significant value to the standard protocols. In literature, it has been noted that joint synergies in gait between stroke patients identify significant differences that cannot be revealed by standard gait analysis [37]. Indeed, kinematic synergy analysis was used in various locomotion tasks [29,38], hand grasps [26,39], and upper limb [30] movements. However, kinematic synergies were extracted only from marker-based tracking data. Kinematic synergies were extracted from Kinect data only by Lambert-Shirzad and colleagues [24,25]. In one study, bilateral hand movements were acquired from the Kinect camera and three different factorization methods were compared for the extraction of kinematic synergies, concluding that PCA and NMF outperformed independent component analysis (ICA) [25]; in the second study, kinematic synergies were compared between healthy and stroke patients, finding that more synergies are needed for stroke patients to achieve the same level of reconstruction accuracy [24]. However, in these studies, joint angles were computed developing a musculoskeletal model in OpenSim and not directly from the skeleton joint positions, and the validity of the kinematic muscle extraction with respect to the gold standard tracking systems was not demonstrated.

Employing a synergistic approach for comparison of the performance between marker-based and markerless systems opens the way to relevant in-depth measurements that include motor control assessments that are becoming crucial in the evaluation of many pathologies, promoting assessments at neural level. Many studies already used kinematic measures, such as articular angles or range of motions, to compare the performance between marker-based and markerless tracking systems. Kinematics of both upper limbs [20] and lower limbs [17,40] computed from markerless sensors was found to have good agreement with kinematics computed from marker-based systems and, therefore, markerless sensors are feasible for assessing human kinematics. Thus, the comparison can be shifted from kinematic measures to kinematic synergies, providing insight also on the synergistic control, which was not assessed before.

In this study, kinematic synergies were used as benchmark metrics for evaluating the performance of markerless systems. Kinematic synergies were extracted from tracking data of a markerless system in order to quantitatively demonstrate its range of application with respect to the gold standard systems, using the data from fifteen participants performing multi-directional upper limb movements.

2. Materials & methods

2.1. Participants

Fifteen healthy participants (8 females, 7 males, mean age 24.0 ± 3.0 years) were recruited for this study with no musculoskeletal impairments affecting their performance. Ethical approval was granted by the CNR Ethical Committee (Rome, Italy, protocol number 0044338/2018) and the experimental trial was conducted in compliance with the Declaration of Helsinki. The participants provided written informed consent to participate in this study and for the publication of any data included in this article.

2.2. Acquisition setup

Kinematic data were recorded with both a marker-based, optoelectronic system (Vicon, Vicon Motion Systems, Oxford, UK) and a markerless tracking system (Kinect V2, Microsoft, Redmond, WA, USA). Kinect V2 was used as it is a well-known and documented markerless system for motion tracking [7,15,41]. Although a new generation of Kinect sensors was launched, recent studies have demonstrated that Kinect V2 performances are comparable to those achieved with the recent Kinect Azure in both upper limb tracking accuracy [14] and in shoulder angle estimation [42]. The Vicon system featured 10 infrared cameras, and the Vicon Upper Limb model consisted of 25 retroreflective markers placed on specific anatomical landmarks. To improve the accuracy and reliability of the tracked data of the markerless sensor, our software for acquisition provided real time monitoring of the tracked and inferred joints and only tracked data were considered. Moreover, the Kinect was placed following the Microsoft's suggestions. The Kinect V2 camera was placed in front of the participant at about 2.0 m, at a height of approximately 1.5 m. Participants were instructed to perform a set of point-to-point movements, as motion primitives for daily life activities, following a similar protocol previously adopted for muscle synergy studies [43]. Movements consisted in reaching 9 targets on a circular board. Eight targets were placed at 8 cardinal points (North-East (NE), East (E), South-East (SE), South (S), South-West (SW), West (W), North-West (NW), North(N)) and one in the center of the board (labelled as O). Movements started from a reference position with the arm leaning along the body. First of all, the participant reached the point O from the reference position and went back to the initial position; then, all the other points were reached with the same modality. The target board was positioned according to 3 different orientation in order to include a more comprehensive volume of the upper limb workspace: laterally on the right (Right), frontally in horizontal position (Horizontal), and laterally on the left (Left). Each set of movements was performed with the right arm and was repeated twice and recorded simultaneously with the marker-based and markerless systems. The set-up for the acquisition is the same described in Scano et al. [21] and it is shown in Fig. 1.

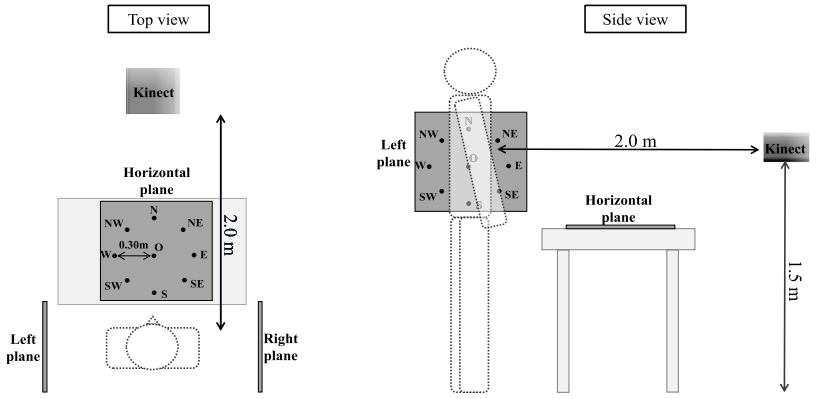

Fig. 1. Setup for the acquisition. Position of the markerless system with respect to the participant is reported from the top view (left panel) and from the lateral view (right panel). The three positions of the target are shown (horizontal, right, left) in both view; in the lateral view, the right panel is not shown for representation purposes.

2.3. Signal processing

Vicon data consisted in 3D marker trajectories. They were sampled at 100 Hz and labelled in the Vicon Nexus software. The joint center of movement of shoulder, elbow, and wrist was reconstructed with the Vicon Upper Limb model for both the right and left arm. Kinect data consisted in 3D trajectories of 25 joints of the Microsoft SDK 2.0 skeleton, sampled at 30 Hz. Both marker-based and markerless data were filtered with a 3rd order low-pass Butterworth filter with cut-off frequency = 5 Hz, a typical cut-off frequency for kinematics [14,23,44]. Movements were segmented with a threshold algorithm on the time series of the velocity of the wrist. Forward phases (from the reference position to the target) and backward phases (from the target to the reference position) were identified for each movement. The onset and the offset of the phases were computed when wrist velocity exceeded the 5 % of the maximum absolute velocity of the wrist. Only the forward phases were considered for the analysis, as it is typically done in similar work regarding synergistic approaches. In fact, in forward phases, kinematic patterns are due to phasic muscle activity rather than relying on gravity [45].

Ten rotational degrees of freedom (DoFs) of the upper limb and upper body were computed from the position of the centers of rotation of the right upper limb, described in detail in Scano et al. [21]. In particular, DoFs considered were the shoulder elevation, shoulder plane of elevation, shoulder internal-external rotation (positive internal rotation), elbow flexion-extension, hand flexion-extension, hand deviation (positive radial deviation), scapular elevation, trunk torsion, trunk antero-posterior flexion, trunk medio-lateral flexion. All variables were computed in the subject specific reference system. In appendix A, equations for DoF computation are reported. All the time series of the forward phases of the DoF were segmented and each phase was resampled at 100 samples in order to allow comparison between phases and participants.

2.4. Synergy extraction

Kinematic synergies were extracted separately from the makerless and marker-based datasets. The synergy extraction procedure consists in decomposing the input signals in time-invariant vectors (synergies) and in corresponding time-varying coefficients that modulate the activations of the synergy in the different movement phases. In this study, kinematic synergy extraction was performed with the Mixed-Matrix factorization (MMF) algorithm [32], that extends the standard Non Negative Matrix Factorization, allowing to decompose signals with negative components. All repetitions and board orientation were concatenated in a single matrix. Therefore, for each participant, the DoFs were arranged in a matrix with M rows and $K \bullet T \bullet R$ columns, where M is the number of DoF and K is the number of tasks sampled with T samples each and R is the number of repetitions. In this study, $K = 9 \bullet 3$, $T = 100$, $R = 2$, $M = 10$. Thus, input data was a 10×5400 matrix. The MMF algorithm decomposes the input signal as:

$$KIN(t,k,r,m) = \sum_{i=1}^{S} c_i^{k,r}(t)\, \boldsymbol{w_i}(m)$$

where $\boldsymbol{w_i}$ are the time-invariant synergy vectors and $\boldsymbol{c_i}$ the time-varying scalar activation coefficients for each synergy ($i = 1 \ldots S$), and $KIN(t,k,r,m)$ the angle of the DoF m at time t of repetition r in task k. Synergy extraction leads to the identification of S synergies (each a column vector with 10 components) and $S \bullet 5400$ time-varying coefficients. Each spatial synergy was normalized by the Euclidean norm of that synergy and the temporal coefficients were normalized by the reciprocal of the norm. Therefore, in this synergy model, the original signal KIN can be reconstructed by multiplying the synergy matrix W by the matrix of the temporal coefficients C. To evaluate the quality of reconstruction of the input signal, the reconstruction R^2 was computed as $1 - \frac{SSE}{SST}$ where SSE is the sum of the squared residuals and SST is the sum of the squared differences with the mean KIN vector [43]. The kinematic synergies were extracted from 1 to 10 number of synergies and the algorithm was repeated 20 times in order to avoid local minima and, for each number of synergies, the solution with the highest R^2 was chosen. Since multiple criteria have been used in literature for the choice of the optimal number of synergies to extract, we extracted the same number of synergies from each participant to allow inter-individual comparison. The number of synergies were chosen as the lowest one that allow to reach at least the mean R^2 (computed across participants) > 0.90.

2.5. Synergy clustering

In order to identify synergistic patterns common to all participants, synergies were grouped with the k-means clustering algorithm [46]. The set of kinematic synergies extracted from all the participants was used as input to the clustering algorithm and the number of clusters was increased from the number of extracted synergies until all synergies from the same participant were grouped in different clusters. The algorithm was repeated 200 times with a new initialization of initial centroids (mean synergy for each of the clusters) at each iteration with the same number of clusters and the solution that minimized the sum of Euclidean distances of each synergy with respect to the centroids was chosen. The procedure was done separately for marker-based and markerless datasets.

2.6. Outcome measures and statistics

The quality of the reconstruction was quantified with the R^2 value for each dataset (marker-based and markerless). Each dataset was tested for normality using the Kolmogorov-Smirnov test and the R^2 was compared with paired t-tests for each number of synergies. The level of significance (α) was set 0.05. The Bonferroni correction for multiple comparisons was adopted. Thus, since ten tests were performed, the α level was $\alpha_{corrected} = \alpha/10 = 0.005$.

The number of synergies to extract from each participant was defined as the lowest one for which the reconstruction $R^2 > 0.90$. For each participant, synergies were matched by similarity between marker-based and markerless datasets and inter-subject similarity was computed as the cosine angle between matched synergies for the spatial synergies and as the Pearson's correlation coefficients between the corresponding temporal coefficients.

To evaluate the variability of synergies across participants, the mean intra-cluster similarity was computed as the mean similarity found across all the possible pairs of synergies belonging to the cluster. Similarity between spatial synergies was evaluated with the cosine angle, while similarity between temporal coefficients was computed as correlation coefficients.

Finally, clusters from marker-based and markerless datasets were matched for similarity and inter-cluster similarity was computed between matched clusters with cosine angle for spatial synergies and with correlation coefficients for temporal coefficients.

3. Results

3.1. Articular angles

In Fig. 2, mean angles computed from the tracked data of the two systems are shown. The mean angle errors for each DOF are $\leqslant 5^\circ$ in all sectors, except for the shoulder plane of elevation, shoulder internal/external rotation, hand deviation, and hand flexion that are between 5° and 15°. These results confirmed the errors that were found in the previous study with the same setup [21].

3.2. Reconstruction R^2

In Fig. 3, the comparison of the reconstruction R^2 for the marker-based and markerless datasets is shown.

The reconstruction R^2 was not statistically different when comparing marker-based and markerless datasets ($p > 0.005$, due to Bonferroni correction). The mean R^2 exceeded 0.90 at 4 synergies with $R^2 = 0.94$ for both marker-based and markerless datasets. Therefore, 4 synergies were extracted from each subject.

3.3. Synergy extraction

In Fig. 4, an example of 4 kinematic synergies extracted from subject 1 is shown for marker-based and markerless datasets. Synergies were matched by similarity. The corresponding temporal coefficients are reported in Fig. 5.

In Fig. 6, an example of the original input signal and the reconstructed signal, computed as W•C with 4 synergies is shown for marker-based data.

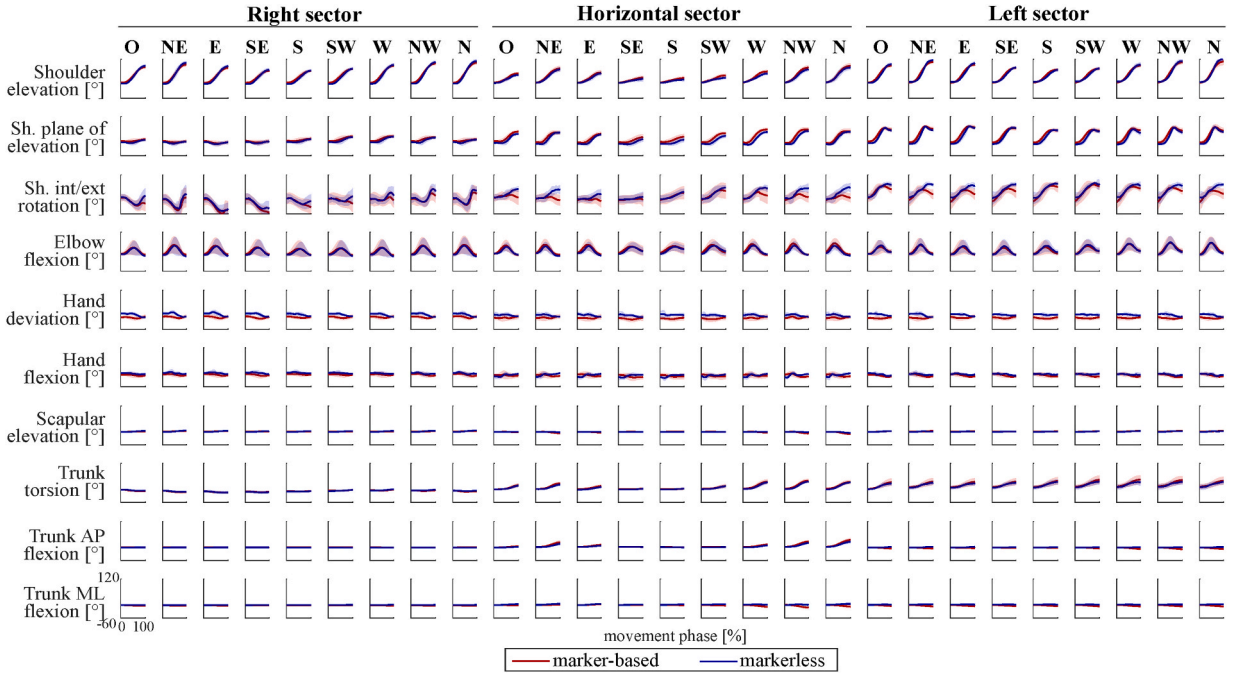

Fig. 2. Articular angles. Means and standard deviations of the 10 DOFs considered are reported for marker-based (in red) and markerless (in blue) datasets. Each movement phase is reported in columns, while the DOFs (angles in °) are reported in rows. Column Labels indicate the direction of motion: 0: center of the target; NE: North-East direction; E = East; SE = South-East; S = South; SW = South-West; W = West; NW = North-West; N = North. (For interpretation of the references to colour in this figure legend, the reader is referred to the Web version of this article.)

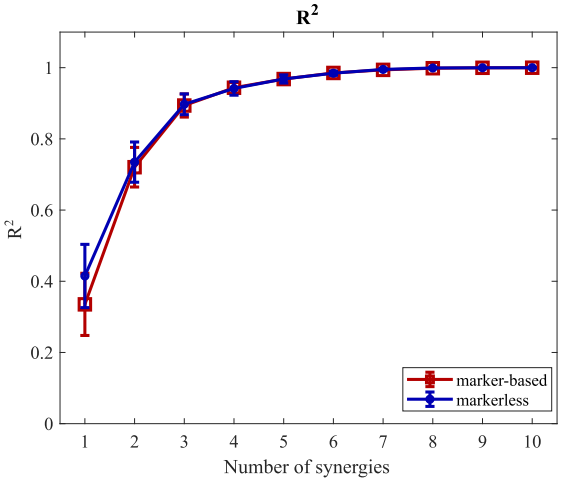

Fig. 3. Reconstruction R^2. Comparison between reconstruction R^2 of marker-based data (red) and markerless data (blue). The squares and the circles are the mean R^2 across participants (marker-based and markerless, respectively) and the error bars represent the standard deviations. (For interpretation of the references to colour in this figure legend, the reader is referred to the Web version of this article.)

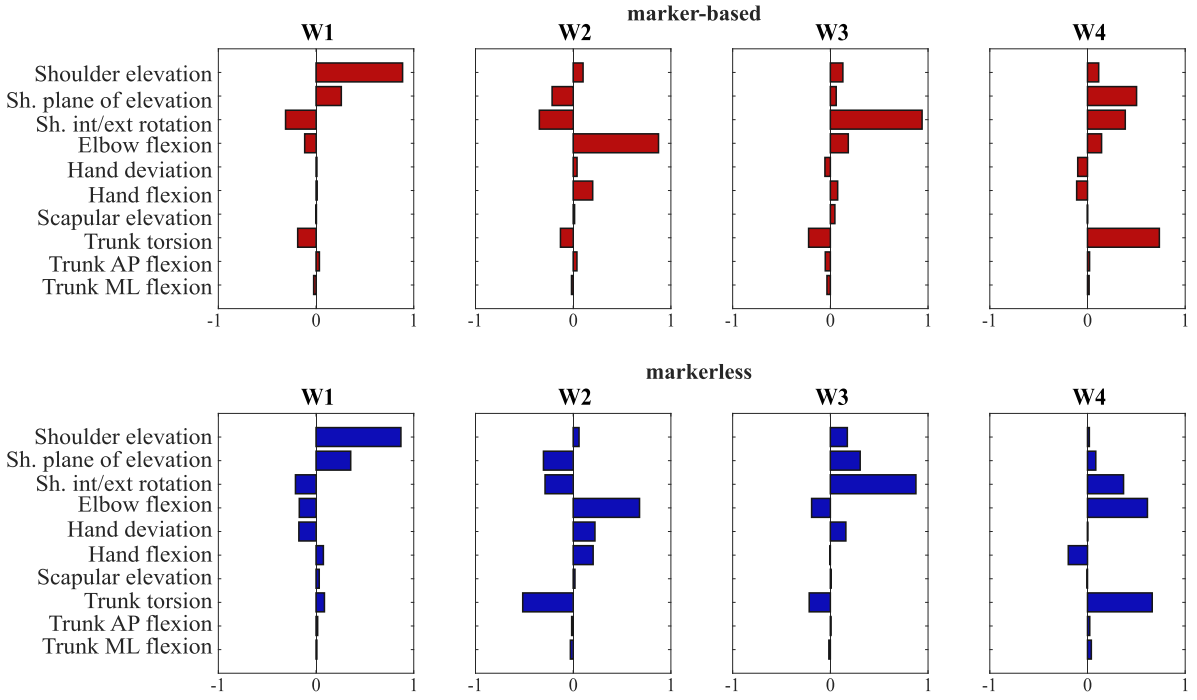

Fig. 4. Kinematic synergies. Example of kinematic synergies extracted from the marker-based (upper panel in red) and the markerless (lower panel in blue) datasets for one participant. Synergies were matched by similarity. (For interpretation of the references to colour in this figure legend, the reader is referred to the Web version of this article.)

In Fig. 7, an example of the original signal and the reconstructed signal with 4 synergies is shown for markerless data.

In Table 1, intra-subject similarity of matched synergies and temporal coefficients between marker-based and markerless datasets are reported.

Matched synergies showed a quite high to very high cosine similarity (>0.60) for the first three synergies, except for subject 8, while the last synergy showed lower similarity, even <0 for some participants. Similarity of matched temporal coefficients, instead, was different for each participant and, in some cases, did not correspond to the same trend of the similarity of the synergies.

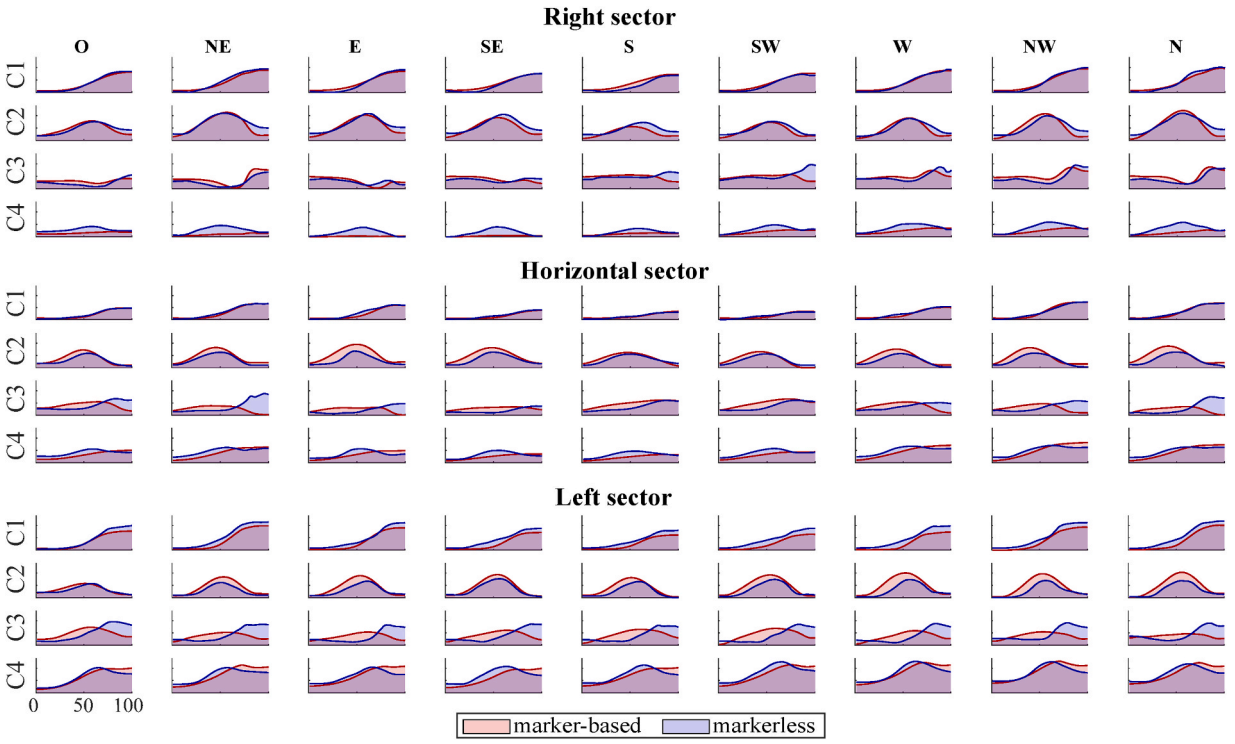

Fig. 5. Temporal coefficients. Temporal coefficients extracted from the marker-based (in red) and the markerless (in blue) datasets for one participant. Temporal coefficients were matched based on synergy similarity. Movement phases are reported in columns, temporal coefficients C in rows for Right (first panel), Horizontal (second panel), and Left (last panel) movements. Column Labels indicate the direction of motion: 0: center of the target; NE: North-East direction; E = East; SE = South-East; S = South; SW = South-West; W = West; NW = North-West; N = North. Repetitions are averaged for visualization purposes. (For interpretation of the references to colour in this figure legend, the reader is referred to the Web version of this article.)

3.4. Synergy clustering

In Fig. 8, the results of the clustering procedure are shown for the marker-based system and the markerless system datasets and the corresponding temporal coefficients are reported in Fig. 9. In the marker-based dataset, 12 synergies were grouped in W1, 7 synergies in W2 and W3, 15 synergies in W4, 11 synergies in W5 and 8 synergies in W6. In the markerless dataset, 6 synergies were grouped in W1, 12 synergies in W2, 7 synergies in W3, 14 synergies in W4, 10 synergies in W5 and 11 synergies in W6.

The first cluster W1 is characterized by a negative component of shoulder rotation associated with positive shoulder elevation and elbow flexion. The temporal activation C1 increases during the movement phase, with a maximum before the end of the phase, and it is higher in the Right sector. W2 was characterized by positive shoulder elevation and C2 increased with during the movement, representing the shoulder elevation needed to reach the target. W3 shows positive shoulder plane of elevation, rotation and trunk torsion that was more active in the Left sector. W4 is characterized by the positive elbow flexion that has maximum activation at the half of the movement phase. W5 shows positive rotation coupled with positive shoulder elevation for marker-based data and with negative plane of elevation and positive elbow flexion for markerless data. C5 shows that the fifth cluster activates more at the end of the phase, except for the Horizontal sector in which the activation is almost constant. Finally, W6 is characterized by positive shoulder rotation and elbow flexion and negative hand deviation and hand flexion for marker-based data that is active more at the half of the movement phase and by positive shoulder elevation and rotation that is activated principally at the end of the phase.

In Table 2, the similarity across synergies of the same clusters is reported for both Vicon and Kinect datasets. The similarity between matched clusters from marker-based and markerless datasets are also reported.

Good similarity was found in each cluster of the spatial synergies for both marker-based and markerless data, while clusters of the temporal coefficients showed high similarity (>0.70) in five clusters, moderate similarity in one cluster (0.54) and low similarity (<0.50) in 6 clusters. The mean intra-cluster similarity was 0.75 (0.04) for marker-based data and 0.77 (0.03) for markerless data. The average similarity of random chosen pairs of synergies extracted was 0.15 (0.47) for marker-based data and 0.14 (0.50) for markerless data, so consistently lower than the obtained result. Inter-cluster similarity of matched cluster was high ($\geqslant 0.70$) for the first three cluster, moderate ($\geqslant 0.60$) for W4 and W5, and very low (0.10) for the last cluster. Clusters of temporal coefficients are matched with a high similarity in C1, C2, C3 and C4, moderate in C5 and very low in C6.

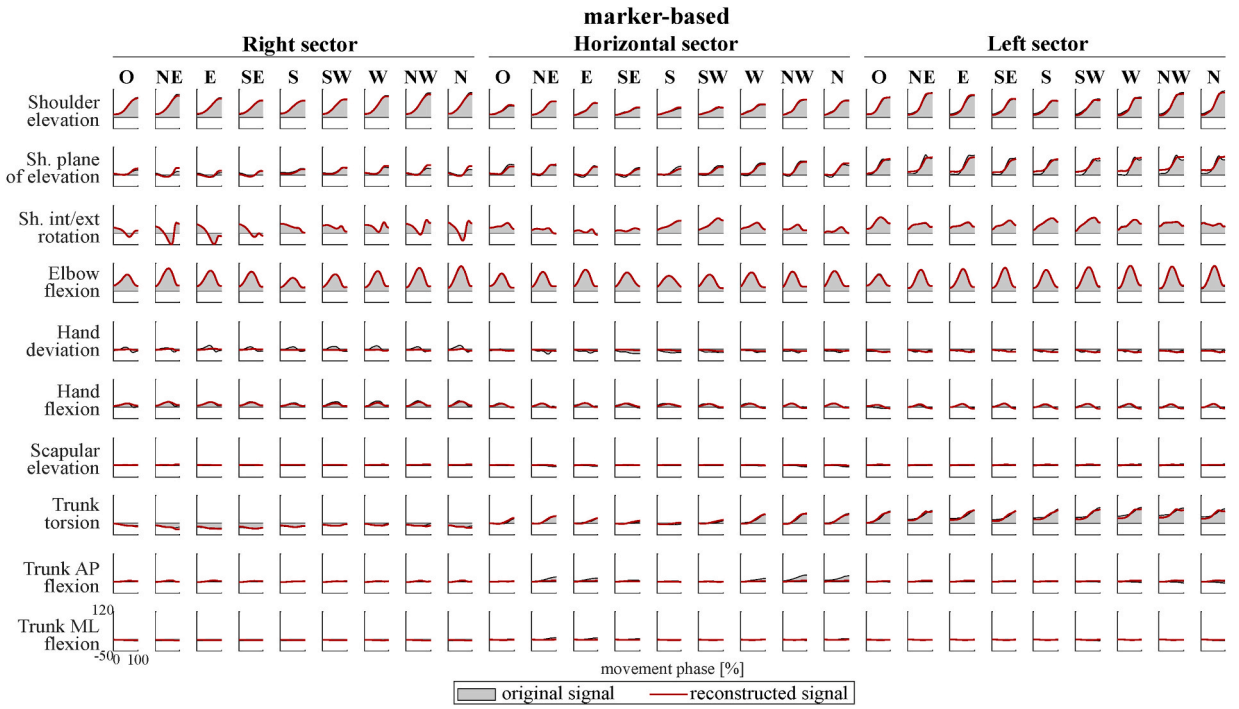

Fig. 6. Marker-based reconstructed signal. Original signal (in gray) and reconstructed signal with 4 synergies (in red) are reported for marker-based data. Each movement phase is reported in columns, while the DoFs (angles in °) are reported in rows. Column Labels indicate the direction of motion: 0: center of the target; NE: North-East direction; E = East; SE = South-East; S = South; SW = South-West; W = West; NW = North-West; N = North. (For interpretation of the references to colour in this figure legend, the reader is referred to the Web version of this article.)

4. Discussion

4.1. Main findings

In this study, kinematic synergies were extracted from 3D joint tracking data of fifteen participants performing upper limb movements in multiple directions during simultaneous recording from the markerless Kinect V2 and the marker-based Vicon system. The extracted kinematic synergies were compared between the two systems. Four synergies were extracted from all participants for both markerless and marker-based data, corresponding to a reconstruction accuracy (R^2) of the original input kinematics waveforms of at least 0.90.

All participants, except one, showed high similarity for at least three synergies between markerless and marker-based data, indicating that markerless systems capture kinematic synergies very similar to the gold standard. These similarities are present also in the temporal coefficients, that showed high correlations between matched synergies. Cluster analysis found six mean synergies for both markerless and marker-based data, showing good intra-cluster similarity (i.e., synergies could be well generalized across subjects). Five clusters were matched with good similarity (⩾60) and only one cluster was not matched well. The first and second cluster describes the negative rotation of the shoulder and the shoulder elevation, respectively. The third cluster represents all the three DoFs of the shoulder and trunk torsion, the forth cluster represents mainly the elbow flexion and the fifth cluster is mainly characterized by the positive shoulder rotation. The last cluster is the most different between marker-based and markerless data: for the data of the marker-based system, the sixth mean synergy is characterized by shoulder rotation and elbow flexion with negative hand flexion and deviation, while for data from the markerless system, the sixth synergy shows shoulder elevation and rotation.

4.2. Markerless vs. marker-based systems for extracting kinematic synergies

Assuming the marker-based system as a gold standard, the differences between the synergies extracted from markerless and marker-based systems may be related to some tracking limitations of the markerless camera. A known limitation of the markerless system regards fine and small range movements that are not always clearly detected. In our tests, trunk movements have a limited range of motion and may have not been clearly computed. Indeed, this limitation can be observed in low correlations between synergies extracted from the two systems in some participants. The main mismatch in these synergies was related to a disagreement in hand flexion or deviation, shoulder internal/external rotation and trunk torsion that cannot be clearly and correctly detected by the markerless sensor. This limitation is reflected in the little contribution of trunk flexion and in some disagreements in trunk torsion between marker-based and markerless data in clusters W1, W4 and W5. Moreover, the tracking of wrist/hand joints are based on few

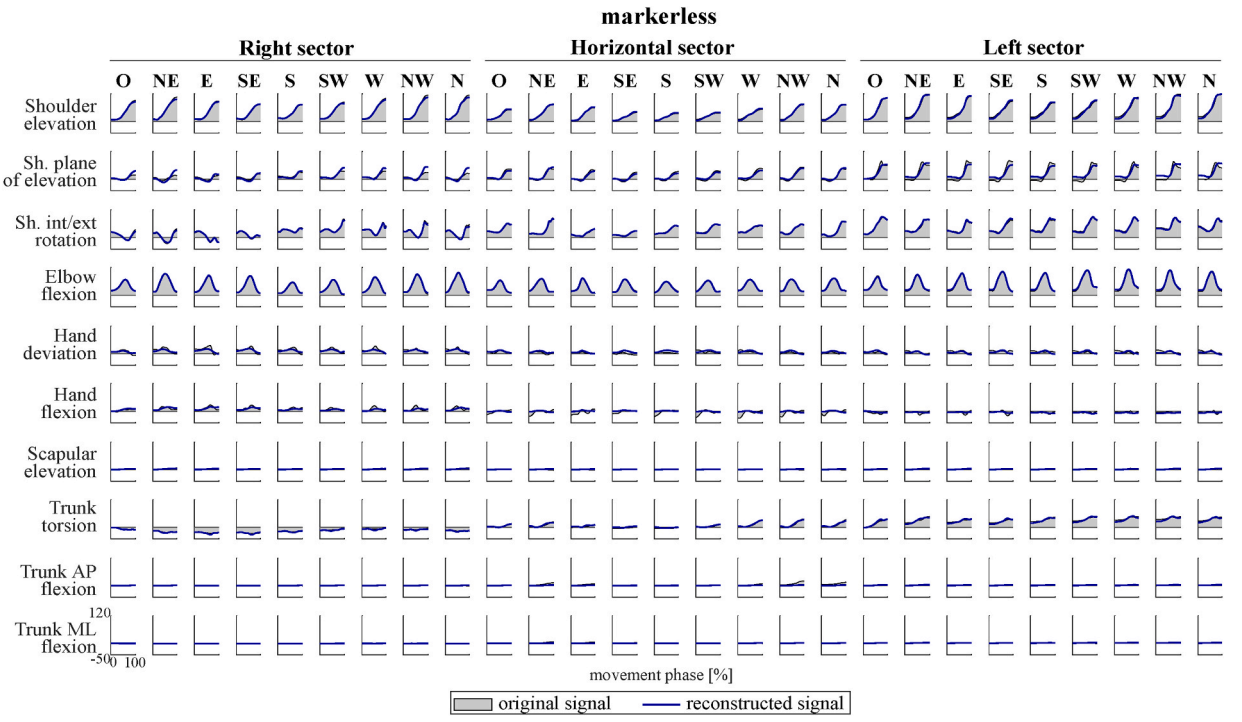

Fig. 7. Markerless reconstructed signal. Original signal (in gray) and reconstructed signal with 4 synergies (in blue) are reported for markerless data. Each movement phase is reported in columns, while the DoFs (angles in °) are reported in rows. Column Labels indicate the direction of motion: 0: center of the target; NE: North-East direction; E = East; SE = South-East; S = South; SW = South-West; W = West; NW = North-West; N = North. (For interpretation of the references to colour in this figure legend, the reader is referred to the Web version of this article.)

Table 1
Intra-subject similarity of matched synergies and temporal coefficients between marker-based and markerless datasets are reported for all 15 participants. Mean and standard deviations for each participant are reported.

Markerless vs. marker-based system: intra-subject similarity															
Kinematic synergies (cosine similarity)															
	S01	S02	S03	S04	S05	S06	S07	S08	S09	S10	S11	S12	S13	S14	S15
W1	0.93	0.82	0.89	0.97	0.89	0.95	0.72	0.81	0.79	0.90	0.99	0.87	0.98	0.90	0.80
W2	0.88	0.82	0.88	0.86	0.79	0.91	0.70	0.72	0.76	0.67	0.95	0.85	0.84	0.89	0.75
W3	0.87	0.81	0.79	0.84	0.70	0.91	0.67	0.22	0.75	0.61	0.93	0.84	0.82	0.85	0.70
W4	0.79	−0.53	0.60	0.71	−0.05	0.86	0.46	−0.33	0.42	−0.14	0.92	0.63	0.30	0.47	0.52
mean	0.87	0.48	0.79	0.84	0.58	0.91	0.64	0.35	0.68	0.51	0.95	0.80	0.74	0.78	0.69
std	0.06	0.67	0.13	0.11	0.43	0.03	0.12	0.53	0.17	0.45	0.03	0.11	0.30	0.20	0.12
Temporal coefficients (Pearson's coefficient)															
C1	0.96	0.18	0.69	0.88	0.89	0.91	0.75	0.94	0.79	0.96	0.98	0.86	0.94	0.76	0.90
C2	0.85	0.83	0.70	0.81	0.87	0.82	0.63	0.73	0.83	0.35	0.79	0.53	0.91	0.93	0.73
C3	0.32	0.81	0.95	0.71	0.74	0.89	0.76	−0.01	0.80	0.74	0.97	0.89	0.82	0.94	0.90
C4	0.92	−0.03	0.61	0.77	0.33	0.70	0.80	0.22	0.61	−0.06	0.77	0.49	0.31	0.70	0.75
mean	0.76	0.45	0.74	0.79	0.71	0.83	0.74	0.47	0.76	0.50	0.88	0.69	0.75	0.83	0.82
std	0.30	0.44	0.15	0.07	0.263	0.10	0.06	0.44	0.10	0.45	0.11	0.21	0.29	0.12	0.09

anatomical landmarks and therefore, estimation of hand/wrist degrees of freedom can be unstable. It follows that hand deviation and flexion may have not been clearly detected, as already observed in previous work [19]. Coherently, we found that in cluster W2, W4 and W5 the hand DoFs of the markerless sensor had higher contributions with respect to the marker-based system, since the instability of hand and wrist joints resulted in wider movements of the hand. The instability of the wrist may influence also the elbow flexion and, therefore, this justifies the higher amplitude of the elbow flexion in W2, W3 and W5 for markerless data with respect to marker-based data. Finally, the arm performing the movement in the Left sector may have occluded some joints as already reported in the literature [47] or the target in the Horizontal sector could have occluded the lower limb affecting the overall accuracy [23]. Despite these sources of errors, the markerless sensor showed to be feasible for the extraction of kinematic synergies.

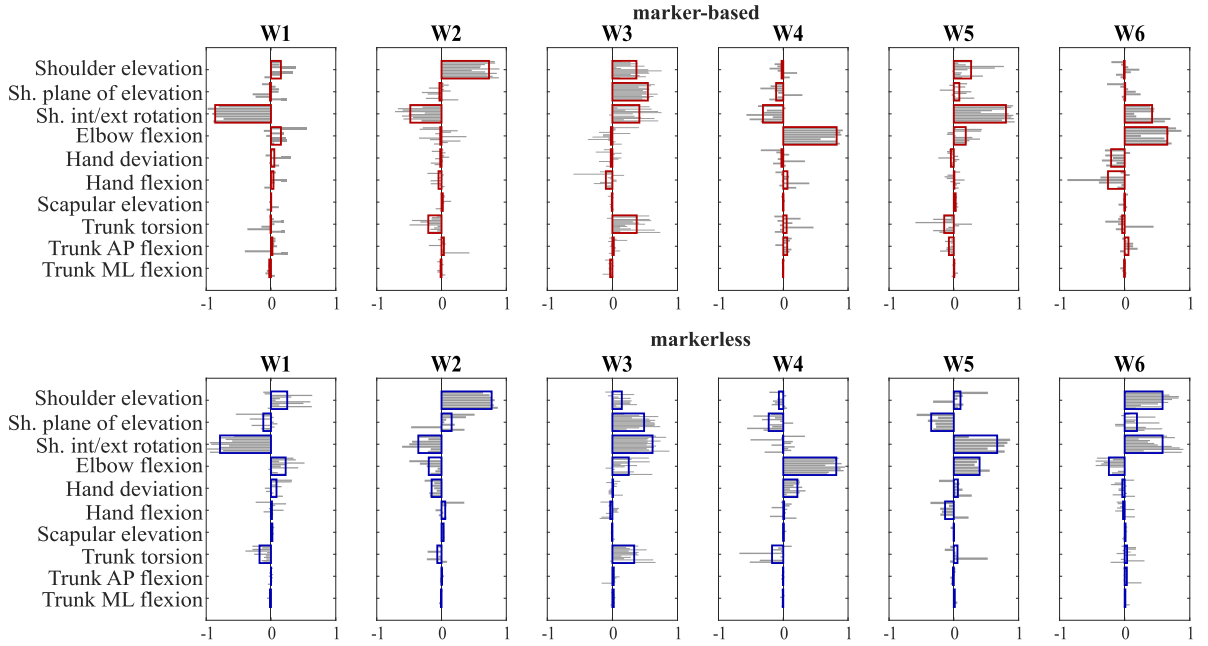

Fig. 8. Synergy clustering. Results of the synergy clustering procedure are reported for marker-based (upper panel in red) and markerless (lower panel in blue) system. Bold lines represent the mean synergy of the cluster while gray lines represent synergies of all participants. (For interpretation of the references to colour in this figure legend, the reader is referred to the Web version of this article.)

4.3. Comparison with previous work based on kinematic synergies in the upper limb

In literature, kinematic synergies were mainly used for the analysis of motor control of hand grasps, since they are the most suitable way for investigating synergistic control when a large number of degrees of freedom is involved, especially on the human hand [26, 39]. However, few studies extracted kinematic synergies in upper limb reaching movements. In a previous study, kinematic synergies were extracted with PCA from data collected with IMU in multi-joint upper limb movements, finding that only 4 synergies were needed to explain the 94 % of the VAF, which is comparable to our results [30]. These 4 synergies represent the main kinematic pattern of the movements and higher order synergies described fine motions of specific phases. Similar results were found also in reach-to-grasp movements in which three synergies reconstructed the 86 % of the total variance by describing the main patterns of the movement, such as elbow flexion, shoulder elevation or shoulder angles related to trunk rotation [48]. Another study, instead, found that only three kinematic synergies are needed to explain the 95 % of variance in manipulation tasks with 12 joints analyzed [49], while we found that four synergies explain about 94 % of the VAF. Lambert-Shirzad & Van der Loos found that 3 to 4 kinematic synergies are needed for explaining the 90 % of the VAF using 10 DoFs [25], similarly to our results. However, their synergies seemed to be less sparse than our synergies and this may be related to the different factorization method used.

4.4. Novelties and applications

The MMF algorithm for kinematic synergy extraction extends the previous factorization algorithms that are usually employed. Since kinematic data can be either positive and negative to represent the extension and the flexion of a joint, the NMF algorithm is not the most suitable way for the extraction of kinematic synergies as it has a constrain of non-negativity of the input data. PCA, instead, allows the factorization of positive and negative data, but it adds a constraint of orthogonality between the extracted synergies that does not adhere to the physiological needs [50]. MMF algorithm is also suitable for performing kinematic synergy extraction by replacing angular displacements with angular velocities or accelerations, since they are positive and negative signals.

This is the first time that the validity of markerless systems is demonstrated and quantified also for motor control analysis with kinematic synergies. Synergies can be used as biomarker for the assessment of neuromotor diseases, such as post-stroke patients, and for the evaluation of the motor recovery. In clinical context, the analysis of synergies (muscle and/or kinematic) assesses how the motor control of patients is altered with respect to healthy subjects. Patients with impaired motor control, such as post-stroke patients and with Parkinson's disease, showed altered synergistic patterns, reflecting an altered motor control. In particular, it has been demonstrated that muscle synergies changes in number and composition with stroke, depending also on the severity of motor impairment [51]. Kinematic synergies may allow to investigate motor control without the need of the EMG signal and with the advent of markerless sensors, this kind of assessment can be carried in domestic context. In this way, the motor control assessment can be performed during telerehabilitation, providing more information than clinical scale only. Kinematic synergies can be used to evaluate

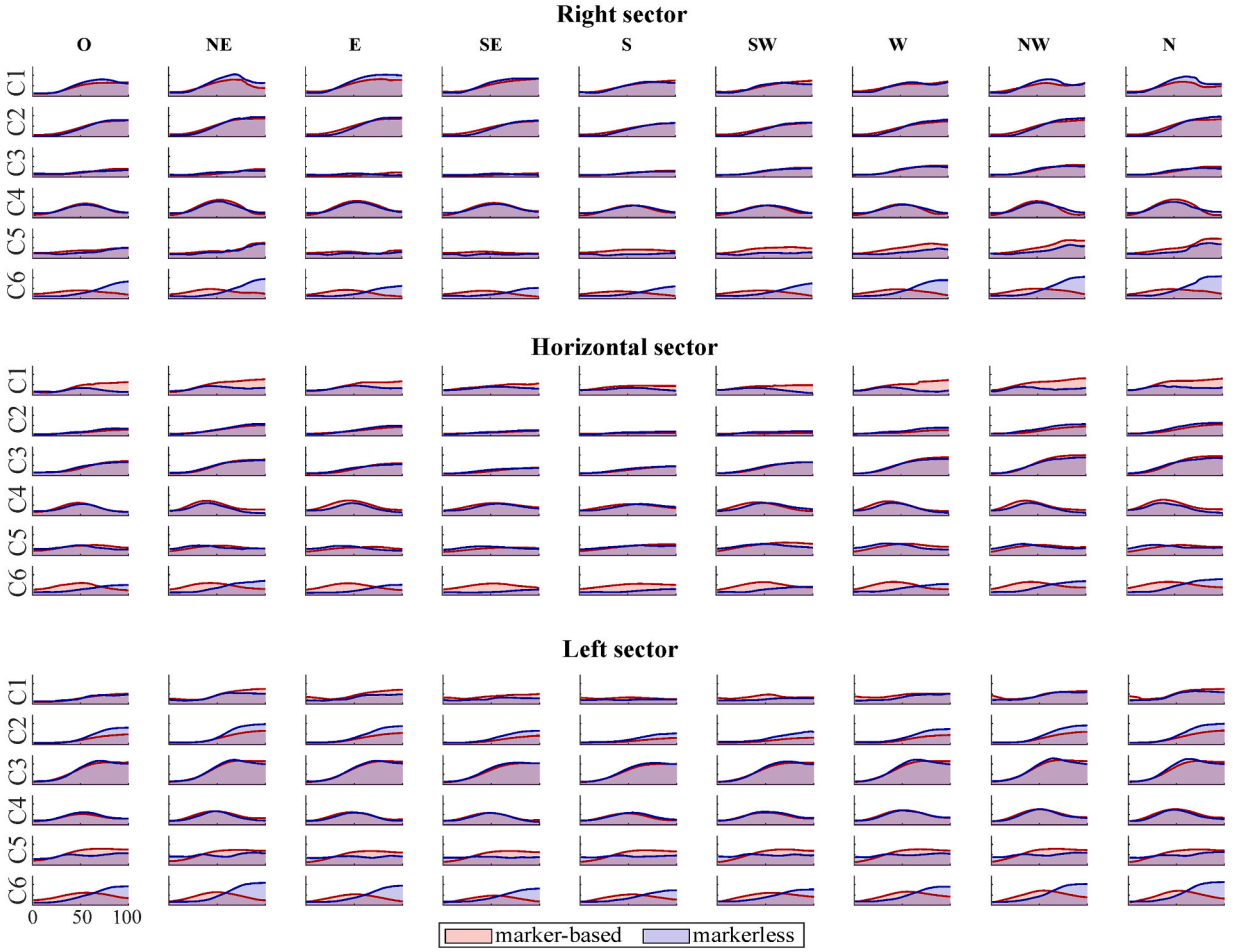

Fig. 9. Temporal coefficients clustering. Mean temporal coefficients of the clusters are reported for marker-based (in red) and markerless (in blue) system. Movement phases are reported in columns, temporal coefficients C in rows for Right (first panel), Horizontal (second panel), and Left (last panel) movements. Column Labels indicate the direction of motion: 0: center of the target; NE: North-East direction; E = East; SE = South-East; S = South; SW = South-West; W = West; NW = North-West; N = North. Repetitions are averaged for visualization purposes. (For interpretation of the references to colour in this figure legend, the reader is referred to the Web version of this article.)

Table 2
Similarity of clustered synergies and temporal coefficients are reported for marker-based and markerless datasets. Mean and standard deviations for each cluster are reported. Inter-cluster similarity is reported between matched clusters for spatial synergies and temporal coefficients.

Intra-cluster cosine similarity (spatial synergies) and Pearson's correlation (temporal coefficients)						
	W1	**W2**	**W3**	**W4**	**W5**	**W6**
marker-based	0.76 (0.13)	0.80 (0.11)	0.74 (0.17)	0.77 (0.19)	0.77 (0.18)	0.67 (0.24)
markerless	0.77 (0.13)	0.79 (0.15)	0.80 (0.15)	0.78 (0.12)	0.72 (0.18)	0.76 (0.14)
	C1	**C2**	**C3**	**C4**	**C5**	**C6**
marker-based	0.28 (0.25)	0.79 (0.12)	0.88 (0.07)	0.48 (0.24)	0.43 (0.23)	0.31 (0.28)
markerless	0.54 (0.23)	0.86 (0.08)	0.88 (0.05)	0.46 (0.19)	0.40 (0.15)	0.73 (0.11)
Kinect vs. Vicon: inter-cluster cosine similarity (spatial synergies) and Pearson's correlation (temporal coefficients)						
Spatial synergies	0.76	0.75	0.70	0.69	0.60	0.10
Temporal coefficients	0.71	0.93	0.99	0.92	0.67	0.004

if the rehabilitation (in clinics or at home) is having positive effects on patients, i.e. they are recovery their motor capability and coordination. In clinics, the motor performance is evaluated with clinical scales, and with some kinematic parameters, like ROM or smoothness metrics. However, this kind of assessments may be subject to biases and low sensitivity and they evaluate the kinematic outcome variables as a result of synergistic coordination. Thus, they cannot describe the underlying modular organization of the motor

control that in neurological patients should be the main focus of interventions [35]. The recovery of physiological motor modules is evidence of motor recovery and, therefore, kinematic synergy analysis adds a significant value to the standard protocols. Moreover, the possibility to use this method with portable tracking systems allows clinicians to assess motor recovery of patients remotely, since only a markerless system is needed.

Therefore, changes in the synergistic patterns can give insights on the motor recovery process of patients. Kinematic synergies reflect joint coordination and how the DOFs are involved in a motor task. Patients with impaired motor control show abnormal movements, that may result in decreased ROM or compensatory strategies, as well as reduced smoothness. All these alterations relate to changes in synergistic patterns with respect to physiological motion. Thus, several groups of patients may show altered synergistic control. Stroke patients have different muscle synergy composition and/or timing, depending on the severity of motor disability [51], and this should reflect in altered kinematic synergies too. In particular, mild patients preserve synergy structures but their activations are altered, while severe post-stroke patients reduce the number of synergies as a result of the merging of motor modules [52]. Patients may show different kinematic synergies because of a reduced ROM in some joints but also because some DOFs may be involved in the task in an abnormal way. This can happen when patients compensate their motor disability with other movements, such as trunk movements, to accomplish a task [53]. Indeed, in patients with impaired motor control, the number of muscle synergies may increase due to a fractionation of the physiological patterns into different modules [51], that can be related to the compensatory motor strategies used to compensate the impaired movement at distal joints [54]. Kinematic synergies, therefore, can identify which DOF is abnormally active, helping in the discrimination of compensatory movements from motor recovery, which sometimes cannot be assessed with clinical scales only [55,56]. Moreover, further studies will investigate at what extent muscle and kinematic synergies relate to each other; using kinematic synergies coupled with low-cost devices might be advantageous in some scenarios due to much faster set-up procedures and the fact that a multi-channel EMG is not needed. The possibility of extracting kinematic synergies from markerless systems paves the way for a more easy and portable application of synergy analysis, allowing to study motor patterns in more flexible scenarios, like in small clinics or at home. In this way, this advanced analysis can be transferred to the clinical routine, avoiding time-consuming setup preparations, saving costs for equipment and trained operators [57]. Therefore, the advance technique of synergy analysis can be performed in fast clinical assessment, accessible for more clinics. Moreover, since no sensors have to be placed on the body, markerless systems are more comfortable for patients, providing a better experience during the assessment [58]. In this way, synergy analysis can be also employed to assess motor control improvements during at home rehabilitation, guaranteeing continuity of care [59]. Furthermore, this can be extended to the coupled analysis of muscular and kinematic signal for the kinematic-muscular synergy extraction [33].

4.5. Limitations and future work

Although the numerous novelties, this study has some limitations. First of all, only ten degrees of freedom of only one upper limb is studied. Future application will include more joints, such as both upper limbs or total body, to make a more comprehensive analysis of the motor control. Moreover, only point-to-point reaching movements were examined. Even though the considered movements include variability since multiple directions and repetitions were included, future work will involve more gestures that can resemble daily life functional movements, such as full body movements, bilateral movements, reaching in more directions, and others. Moreover, more DoFs with a wider range of motion might be included in functional and total body movements. In fact, since kinematic synergies describe how multiple joints are coordinated, the more DOFs are involved in the task, the more comprehensive can be the characterization of movement. Indeed, neurological patients may show impairments in the interlimb coordination and asymmetry in bilateral movements [60,61]. Therefore, including more joints from different limbs in the assessment can provide information also on the interlimb coordination. Then, including also functional movements will provide a description of the motor control in a real scenario, with the only limit of fine manipulation that cannot be evaluated with the Kinect systems. Furthermore, only healthy participants were recruited in this study to assess the performance of the markerless tracking system in the extraction of kinematic synergies. It would be worth to recruit also patients in order to analyze the changes in motor control. Extending the kinematic synergy assessment to patients, in particular those with impaired motor coordination, might give insights on the motor control that cannot be assessed with kinematic data only, as already shown with muscle synergies in stroke [62] and patients with Parkinson's disease [63]. Then, in this study, the Kinect V2 was used as markerless system for motion tracking. However, a new generation of Kinect sensor (Azure Kinect) was released and, therefore, future work may use the new markerless tracking sensors to further improve the tracked data. Finally, multiple technologies could be integrated to compensate the limitations of the markerless sensor, such as IMUs or instrumented gloves, and to extend the analysis to multi-domain variables. Indeed, kinematic data could be associated with muscular data with the extraction of kinematic-muscular synergies [32,33] for a more comprehensive description of the motor control of the upper limb movements.

5. Conclusions

In this study, the performance of a markerless sensor was compared to the gold standard marker-based system with the extraction of kinematic synergies from 10 DoFs computed in multi-direction upper limb movements. The MMF algorithm was used for the extraction of synergies, that allows to factorize positive and negative signals. Good matching was found between synergies extracted from markerlss and from marker-based data, showing that the markerless sensor can be feasible for the kinematic synergy analysis, providing an advanced tool for the evaluation of synergistic control. Our results showed the potentiality of applying synergy analysis to markerless tracking systems, allowing detailed analysis for research in home and clinical scenarios.

Ethics statement

This study was reviewed and approved by the CNR Ethical Committee (Rome, Italy) with protocol number 0044338/2018. All participants provided written informed consent for the use of their data for scientific research purposes.

Data availability statement

The data used in this study will be made available upon reasonable request to the corresponding author.

CRediT authorship contribution statement

Cristina Brambilla: Writing – review & editing, Writing – original draft, Visualization, Validation, Software, Methodology, Investigation, Formal analysis, Data curation, Conceptualization. **Alessandro Scano:** Writing – review & editing, Writing – original draft, Visualization, Validation, Supervision, Software, Resources, Project administration, Methodology, Investigation, Funding acquisition, Formal analysis, Data curation, Conceptualization.

Declaration of competing interest

The authors declare that they have no known competing financial interests or personal relationships that could have appeared to influence the work reported in this paper.

Acknowledgment

The authors wish to thank Robert Mira for his contribution to the work.

Appendix A

Denoting: $\hat{t}$ = vertical unit vector representing the trunk, pointing upwards; $\hat{s}$ = unit vector from left to right shoulder; $\hat{f}$ = unit vector orthogonal to the trunk, pointing forwards; $\hat{a}$ = arm unit vector from shoulder to elbow joint; $\widehat{af}$ = forearm unit vector from elbow to wrist joint; $\hat{n}_1$ = unit vector orthogonal to $\hat{t}$ and $\hat{s}$, pointing forward; $\widehat{n_2}$ = unit vector orthogonal to $\hat{n}_1$ and $\hat{t}$, pointing laterally; $\hat{w}_2$ = unit vector connecting medial to lateral styloid; $\hat{w}_1$ = unit vector orthogonal to $\hat{w}_2$ and $\widehat{af}$; $\hat{h}_1$ = hand unit vector from wrist to hand joint; $\hat{h}_2$ = unit vector orthogonal to $\hat{h}_1$, pointing medially; $\widehat{ap}$ = arm vector projected on a plane orthogonal to the vector $\hat{t}$; $\widehat{af_p}$ = forearm vector projected on a plane orthogonal to the vector $\hat{a}$; $\hat{u}_{hand\Phi}$ = projection of $\hat{h}_1$ on the plane orthogonal to the vector $\hat{w}_1$; $\hat{u}_{hand_\pi}$ = projection of $\hat{h}_1$ on a plane orthogonal to the vector $\hat{w}_2$; $\hat{s}'$ is the vector connecting the trunk to the right glenohumeral joint center projected on the plane orthogonal to the vector $\hat{f}$; $\hat{t}_{sag}$ = projection of vector $\hat{t}$ on the sagittal plane, orthogonal to the vector $\hat{s}$ in the first frame; $\hat{t}_{front}$ = projection of vector $\hat{t}$ on the frontal plane, orthogonal to the vector $\hat{f}$ in the first frame.

$$shoulder\ elevation = \mathrm{acos}(\hat{a} \bullet (-\hat{t}))$$

$$shoulder\ plane\ of\ elevation = \mathrm{acos}[\widehat{ap} \bullet (-\hat{f})] - 90$$

$$shoulder internal \Big/ external rotation = \mathrm{acos}\left(\widehat{af_p} \bullet \widehat{n_2}\right) - 90$$

$$elbow\ flexion = \mathrm{acos}(\hat{a} \bullet \widehat{af})$$

$$hand\ deviation = \mathrm{acos}(\hat{u}_{hand\Phi} \bullet \hat{w}_2) - 90$$

$$hand\ flexion = \mathrm{acos}(\hat{u}_{hand_\pi} \bullet \hat{w}_1) - 90$$

$$scapular\ elevation = \mathrm{acos}(\hat{s}' \bullet \hat{s})$$

$$trunk\ torsion = \mathrm{acos}[\hat{s} \bullet (-\hat{f})] - 90$$

$$trunk antero \Big/ posterior flexion = \mathrm{acos}\left(\hat{t}_{sag} \bullet \hat{f}\right)$$

$$trunk medio \Big/ lateral\ flexion = \mathrm{acos}\left[\hat{t}_{front} \bullet (-\hat{s})\right] - 90$$

References

[1] W.W.T. Lam, Y.M. Tang, K.N.K. Fong, A systematic review of the applications of markerless motion capture (MMC) technology for clinical measurement in rehabilitation, J. NeuroEng. Rehabil. 20 (2023) 57, https://doi.org/10.1186/s12984-023-01186-9.
[2] A.-A. Liu, W.-Z. Nie, Y.-T. Su, L. Ma, T. Hao, Z.-X. Yang, Coupled hidden conditional random fields for RGB-D human action recognition, Signal Process. 112 (2015) 74–82, https://doi.org/10.1016/j.sigpro.2014.08.038.
[3] Z. Liu, H. Qin, S. Bu, M. Yan, J. Huang, X. Tang, J. Han, 3D real human reconstruction via multiple low-cost depth cameras, Signal Process. 112 (2015) 162–179, https://doi.org/10.1016/j.sigpro.2014.10.021.
[4] S. Baffert, N. Hadouiri, C. Fabron, F. Burgy, A. Cassany, G. Kemoun, Economic evaluation of telerehabilitation: systematic literature review of cost-utility studies, JMIR Rehabil Assist Technol 10 (2023) e47172, https://doi.org/10.2196/47172.
[5] Y. Liao, A. Vakanski, M. Xian, D. Paul, R. Baker, A review of computational approaches for evaluation of rehabilitation exercises, Comput. Biol. Med. 119 (2020) 103687, https://doi.org/10.1016/j.compbiomed.2020.103687.
[6] N.K. Mangal, A.K. Tiwari, A review of the evolution of scientific literature on technology-assisted approaches using RGB-D sensors for musculoskeletal health monitoring, Comput. Biol. Med. 132 (2021) 104316, https://doi.org/10.1016/j.compbiomed.2021.104316.
[7] B. Milosevic, A. Leardini, E. Farella, Kinect and wearable inertial sensors for motor rehabilitation programs at home: state of the art and an experimental comparison, Biomed. Eng. Online 19 (2020) 25, https://doi.org/10.1186/s12938-020-00762-7.
[8] A. Ozturk, A. Tartar, B. Ersoz Huseyinsinoglu, A.H. Ertas, A clinically feasible kinematic assessment method of upper extremity motor function impairment after stroke, Measurement 80 (2016) 207–216, https://doi.org/10.1016/j.measurement.2015.11.026.
[9] J. Latorre, C. Colomer, M. Alcañiz, R. Llorens, Gait analysis with the Kinect v2: normative study with healthy individuals and comprehensive study of its sensitivity, validity, and reliability in individuals with stroke, J. NeuroEng. Rehabil. 16 (2019) 97, https://doi.org/10.1186/s12984-019-0568-y.
[10] J. Behrens, C. Pfüller, S. Mansow-Model, K. Otte, F. Paul, A.U. Brandt, Using perceptive computing in multiple sclerosis - the Short Maximum Speed Walk test, J. NeuroEng. Rehabil. 11 (2014) 89, https://doi.org/10.1186/1743-0003-11-89.
[11] B. Galna, G. Barry, D. Jackson, D. Mhiripiri, P. Olivier, L. Rochester, Accuracy of the Microsoft Kinect sensor for measuring movement in people with Parkinson's disease, Gait Posture 39 (2014) 1062–1068, https://doi.org/10.1016/j.gaitpost.2014.01.008.
[12] R. Clark, Y. Pua, K. Fortin, C. Ritchie, K. Webster, L. Denehy, A. Bryant, Validity of the Microsoft Kinect for assessment of postural control, Gait Posture 36 (2012), https://doi.org/10.1016/j.gaitpost.2012.03.033.
[13] R. Clark, Y. Pua, C. Oliveira, K. Bower, S. Thilarajah, R. McGaw, K. Hasanki, B. Mentiplay, Reliability and concurrent validity of the Microsoft Xbox One Kinect for assessment of standing balance and postural control, Gait Posture 42 (2015), https://doi.org/10.1016/j.gaitpost.2015.03.005.
[14] J.A. Albert, V. Owolabi, A. Gebel, C.M. Brahms, U. Granacher, B. Arnrich, Evaluation of the pose tracking performance of the azure Kinect and Kinect v2 for gait analysis in comparison with a gold standard: a pilot study, Sensors 20 (2020) 5104, https://doi.org/10.3390/s20185104.
[15] M. Eltoukhy, J. Oh, C. Kuenze, J. Signorile, Improved kinect-based spatiotemporal and kinematic treadmill gait assessment, Gait Posture 51 (2017) 77–83, https://doi.org/10.1016/j.gaitpost.2016.10.001.
[16] T.M. Guess, R. Bliss, J.B. Hall, A.M. Kiselica, Comparison of Azure Kinect overground gait spatiotemporal parameters to marker based optical motion capture, Gait Posture 96 (2022) 130–136, https://doi.org/10.1016/j.gaitpost.2022.05.021.
[17] M. Wochatz, N. Tilgner, S. Mueller, S. Rabe, S. Eichler, M. John, H. Völler, F. Mayer, Reliability and validity of the Kinect V2 for the assessment of lower extremity rehabilitation exercises, Gait Posture 70 (2019) 330–335, https://doi.org/10.1016/j.gaitpost.2019.03.020.
[18] G. Faity, D. Mottet, J. Froger, Validity and reliability of Kinect v2 for quantifying upper body kinematics during seated reaching, Sensors 22 (2022), https://doi.org/10.3390/s22072735.
[19] K. Otte, B. Kayser, S. Mansow-Model, J. Verrel, F. Paul, A.U. Brandt, T. Schmitz-Hübsch, Accuracy and reliability of the Kinect version 2 for clinical measurement of motor function, PLoS One 11 (2016), https://doi.org/10.1371/journal.pone.0166532.
[20] L. Cai, Y. Ma, S. Xiong, Y. Zhang, Validity and reliability of upper limb functional assessment using the Microsoft kinect V2 sensor, Appl. Bionics Biomech. 2019 (2019) 7175240, https://doi.org/10.1155/2019/7175240.
[21] A. Scano, R.M. Mira, P. Cerveri, L. Molinari Tosatti, M. Sacco, Analysis of upper-limb and trunk kinematic variability: accuracy and reliability of an RGB-D sensor, Multimodal Technologies and Interaction 4 (2020) 14, https://doi.org/10.3390/mti4020014.
[22] P. Plantard, A. Muller, C. Pontonnier, G. Dumont, H.P.H. Shum, F. Multon, Inverse dynamics based on occlusion-resistant Kinect data: is it useable for ergonomics? Int. J. Ind. Ergon. 61 (2017) 71–80, https://doi.org/10.1016/j.ergon.2017.05.010.
[23] C. Brambilla, R. Marani, L. Romeo, M. Lavit Nicora, F.A. Storm, G. Reni, M. Malosio, T. D'Orazio, A. Scano, Azure Kinect performance evaluation for human motion and upper limb biomechanical analysis, Heliyon 9 (2023) e21606, https://doi.org/10.1016/j.heliyon.2023.e21606.
[24] N. Lambert-Shirzad, H.F.M. Van der Loos, Data sample size needed for analysis of kinematic and muscle synergies in healthy and stroke populations, IEEE Int Conf Rehabil Robot 2017 (2017) 777–782, https://doi.org/10.1109/ICORR.2017.8009342.
[25] N. Lambert-Shirzad, H.F.M. Van der Loos, On identifying kinematic and muscle synergies: a comparison of matrix factorization methods using experimental data from the healthy population, J. Neurophysiol. 117 (2017) 290–302, https://doi.org/10.1152/jn.00435.2016.
[26] N.J. Jarque-Bou, A. Scano, M. Atzori, H. Müller, Kinematic synergies of hand grasps: a comprehensive study on a large publicly available dataset, J. NeuroEng. Rehabil. 16 (2019) 63, https://doi.org/10.1186/s12984-019-0536-6.
[27] M. Santello, M. Flanders, J.F. Soechting, Postural hand synergies for tool use, J. Neurosci. 18 (1998) 10105–10115, https://doi.org/10.1523/JNEUROSCI.18-23-10105.1998.
[28] M. Santello, G. Baud-Bovy, H. Jörntell, Neural bases of hand synergies, Front. Comput. Neurosci. 7 (2013) 23, https://doi.org/10.3389/fncom.2013.00023.
[29] B. Huang, C. Xiong, W. Chen, J. Liang, B.-Y. Sun, X. Gong, Common kinematic synergies of various human locomotor behaviours, R. Soc. Open Sci. 8 (2021) 210161, https://doi.org/10.1098/rsos.210161.
[30] S. Tang, L. Chen, M. Barsotti, L. Hu, Y. Li, X. Wu, L. Bai, A. Frisoli, W. Hou, Kinematic synergy of multi-DoF movement in upper limb and its application for rehabilitation exoskeleton motion planning, Front. Neurorob. 13 (2019). https://www.frontiersin.org/articles/10.3389/fnbot.2019.00099.
[31] D.D. Lee, H.S. Seung, Learning the parts of objects by non-negative matrix factorization, Nature 401 (1999) 788–791, https://doi.org/10.1038/44565.
[32] A. Scano, R.M. Mira, A. d'Avella, Mixed matrix factorization: a novel algorithm for the extraction of kinematic-muscular synergies, J. Neurophysiol. 127 (2022) 529–547, https://doi.org/10.1152/jn.00379.2021.
[33] A. Scano, N. Jarque-Bou, C. Brambilla, M. Atzori, A. D'Avella, H. Müller, Functional synergies applied to a publicly available dataset of hand grasps show evidence of kinematic-muscular synergistic control, IEEE Access 11 (2023) 108544–108560, https://doi.org/10.1109/ACCESS.2023.3321510.
[34] S.A. Safavynia, G. Torres-Oviedo, L.H. Ting, Muscle synergies: implications for clinical evaluation and rehabilitation of movement, Top. Spinal Cord Inj. Rehabil. 17 (2011) 16–24, https://doi.org/10.1310/sci1701-16.
[35] L.H. Ting, H.J. Chiel, R.D. Trumbower, J.L. Allen, J.L. McKay, M.E. Hackney, T.M. Kesar, Neuromechanical principles underlying movement modularity and their implications for rehabilitation, Neuron 86 (2015) 38–54, https://doi.org/10.1016/j.neuron.2015.02.042.
[36] A. d'Avella, P. Saltiel, E. Bizzi, Combinations of muscle synergies in the construction of a natural motor behavior, Nat. Neurosci. 6 (2003) 300–308, https://doi.org/10.1038/nn1010.
[37] I. Milovanović, D.B. Popović, Principal component analysis of gait kinematics data in acute and chronic stroke patients, Comput. Math. Methods Med. 2012 (2012), https://doi.org/10.1155/2012/649743.
[38] B.J. Stetter, M. Herzog, F. Möhler, S. Sell, T. Stein, Modularity in motor control: similarities in kinematic synergies across varying locomotion tasks, Frontiers in Sports and Active Living 2 (2020). https://www.frontiersin.org/articles/10.3389/fspor.2020.596063.
[39] N. Jarrassé, A.T. Ribeiro, A. Sahbani, W. Bachta, A. Roby-Brami, Analysis of hand synergies in healthy subjects during bimanual manipulation of various objects, J. NeuroEng. Rehabil. 11 (2014) 113, https://doi.org/10.1186/1743-0003-11-113.

[40] Y. Ma, B. Sheng, R. Hart, Y. Zhang, The validity of a dual Azure Kinect-based motion capture system for gait analysis: a preliminary study, in: 2020 Asia-Pacific Signal and Information Processing Association Annual Summit and Conference (APSIPA ASC), 2020, pp. 1201–1206. https://ieeexplore.ieee.org/document/9306232. (Accessed 4 March 2024).
[41] M. Capecci, M.G. Ceravolo, F. Ferracuti, S. Iarlori, S. Longhi, L. Romeo, S.N. Russi, F. Verdini, Accuracy evaluation of the Kinect v2 sensor during dynamic movements in a rehabilitation scenario, in: 2016 38th Annual International Conference of the IEEE Engineering in Medicine and Biology Society, EMBC), 2016, pp. 5409–5412, https://doi.org/10.1109/EMBC.2016.7591950.
[42] U. Özsoy, Y. Yıldırım, S. Karaşin, R. Şekerci, L.B. Süzen, Reliability and agreement of Azure Kinect and Kinect v2 depth sensors in the shoulder joint range of motion estimation, J. Shoulder Elbow Surg. 31 (2022) 2049–2056, https://doi.org/10.1016/j.jse.2022.04.007.
[43] A. d'Avella, A. Portone, L. Fernandez, F. Lacquaniti, Control of fast-reaching movements by muscle synergy combinations, J. Neurosci. 26 (2006) 7791–7810, https://doi.org/10.1523/JNEUROSCI.0830-06.2006.
[44] J. Sinclair, P.J. Taylor, S.J. Hobbs, Digital filtering of three-dimensional lower extremity kinematics: an assessment, J. Hum. Kinet. 39 (2013) 25–36, https://doi.org/10.2478/hukin-2013-0065.
[45] A. Scano, C. Brambilla, M. Russo, A. d'Avella, Upper limb phasic muscle synergies with negative weightings: applications for rehabilitation, in: 2023 IEEE International Conference on Metrology for eXtended Reality, Artificial Intelligence and Neural Engineering (MetroXRAINE), 2023, pp. 834–839, https://doi.org/10.1109/MetroXRAINE58569.2023.10405697.
[46] J.A. Hartigan, Clustering Algorithms, Wiley, 1975.
[47] L. Cai, D. Liu, Y. Ma, Placement recommendations for single kinect-based motion capture system in unilateral dynamic motion analysis, Healthcare 9 (2021) 1076, https://doi.org/10.3390/healthcare9081076.
[48] J. van Kordelaar, E.E.H. van Wegen, G. Kwakkel, Unraveling the interaction between pathological upper limb synergies and compensatory trunk movements during reach-to-grasp after stroke: a cross-sectional study, Exp. Brain Res. 221 (2012) 251–262, https://doi.org/10.1007/s00221-012-3169-6.
[49] T. Hu, J. Kuehn, S. Haddadin, Identification of human shoulder-arm kinematic and muscular synergies during daily-life manipulation tasks, in: 2018 7th IEEE International Conference on Biomedical Robotics and Biomechatronics (Biorob), 2018, pp. 1011–1018, https://doi.org/10.1109/BIOROB.2018.8487190.
[50] N.A. Turpin, S. Uriac, G. Dalleau, How to improve the muscle synergy analysis methodology? Eur. J. Appl. Physiol. 121 (2021) 1009–1025, https://doi.org/10.1007/s00421-021-04604-9.
[51] V.C.K. Cheung, A. Turolla, M. Agostini, S. Silvoni, C. Bennis, P. Kasi, S. Paganoni, P. Bonato, E. Bizzi, Muscle synergy patterns as physiological markers of motor cortical damage, Proc. Natl. Acad. Sci. U. S. A. 109 (2012) 14652–14656, https://doi.org/10.1073/pnas.1212056109.
[52] D.J. Clark, L.H. Ting, F.E. Zajac, R.R. Neptune, S.A. Kautz, Merging of healthy motor modules predicts reduced locomotor performance and muscle coordination complexity post-stroke, J. Neurophysiol. 103 (2010) 844–857, https://doi.org/10.1152/jn.00825.2009.
[53] M.F. Levin, S.M. Michaelsen, C.M. Cirstea, A. Roby-Brami, Use of the trunk for reaching targets placed within and beyond the reach in adult hemiparesis, Exp. Brain Res. 143 (2002) 171–180, https://doi.org/10.1007/s00221-001-0976-6.
[54] J.P. Dewald, P.S. Pope, J.D. Given, T.S. Buchanan, W.Z. Rymer, Abnormal muscle coactivation patterns during isometric torque generation at the elbow and shoulder in hemiparetic subjects, Brain 118 (Pt 2) (1995) 495–510, https://doi.org/10.1093/brain/118.2.495.
[55] M.F. Levin, J.A. Kleim, S.L. Wolf, What do motor "recovery" and "compensation" mean in patients following stroke? Neurorehabilitation Neural Repair 23 (2009) 313–319, https://doi.org/10.1177/1545968308328727.
[56] T.A. Jones, Motor compensation and its effects on neural reorganization after stroke, Nat. Rev. Neurosci. 18 (2017) 267–280, https://doi.org/10.1038/nrn.2017.26.
[57] R.M. Kanko, E.K. Laende, E.M. Davis, W.S. Selbie, K.J. Deluzio, Concurrent assessment of gait kinematics using marker-based and markerless motion capture, J. Biomech. 127 (2021) 110665, https://doi.org/10.1016/j.jbiomech.2021.110665.
[58] E. Knippenberg, J. Verbrugghe, I. Lamers, S. Palmaers, A. Timmermans, A. Spooren, Markerless motion capture systems as training device in neurological rehabilitation: a systematic review of their use, application, target population and efficacy, J. NeuroEng. Rehabil. 14 (2017) 61, https://doi.org/10.1186/s12984-017-0270-x.
[59] M. Trombini, F. Ferraro, M. Morando, G. Regesta, S. Dellepiane, A solution for the remote care of frail elderly individuals via exergames, Sensors 21 (2021) 2719, https://doi.org/10.3390/s21082719.
[60] M.I. Garry, R.E. van Steenis, J.J. Summers, Interlimb coordination following stroke, Hum. Mov. Sci. 24 (2005) 849–864, https://doi.org/10.1016/j.humov.2005.10.005.
[61] S.A. Combs, E.L. Dugan, E.N. Ozimek, A.B. Curtis, Bilateral coordination and gait symmetry after body-weight supported treadmill training for persons with chronic stroke, Clin. BioMech. 28 (2013) 448–453, https://doi.org/10.1016/j.clinbiomech.2013.02.001.
[62] L. Dipietro, H.I. Krebs, S.E. Fasoli, B.T. Volpe, J. Stein, C. Bever, N. Hogan, Changing motor synergies in chronic stroke, J. Neurophysiol. 98 (2007) 757–768, https://doi.org/10.1152/jn.01295.2006.
[63] M. Ghislieri, M. Lanotte, M. Knaflitz, L. Rizzi, V. Agostini, Muscle synergies in Parkinson's disease before and after the deep brain stimulation of the bilateral subthalamic nucleus, Sci. Rep. 13 (2023) 6997, https://doi.org/10.1038/s41598-023-34151-6.